

Effect of the Backboard on the Pyrolysis Front Morphology of Downward Flame Spread: A Simulation Study

Penghui Sun ^{1, a}, Kuibin Zhou ^{1, b}, and Dayu Li ^{1, c}

¹ College of Safety Science and Engineering, Nanjing Tech University, Nanjing 211816, China.

^a 1448670525@qq.com, ^b kbzhou@njtech.edu.cn, ^c ldy9814@163.com

Abstract. In order to investigate the influence of the backboard on the morphology of the pyrolysis front, this study employed the fire dynamics simulator (FDS) to conduct simulation research, aiming to quantitatively analyze the reasons for the differences in the morphology of the pyrolysis front under two conditions: with and without the backboard. By comparing the surface temperature distribution, flow field, and air entrainment velocity at the bottom of the pyrolysis front made of polymethyl methacrylate (PMMA) under different conditions, it was found that the presence of the backboard not only reduced the surface temperature of PMMA at the bottom of the pyrolysis front and the temperature difference between the edge and middle, but also changed the flow field at the edge and suppressed the horizontal air entrainment velocity at that position, especially for thinner PMMA. These factors ultimately result in a larger angle of the pyrolysis front during the burning stable stage under the condition with the backboard compared to the condition without the backboard. In addition, the trend of horizontal air entrainment velocity at the edge position under different conditions also provide data support for the qualitative observation and analysis of previous experiments phenomena.

Keywords: Downward flame spread; Pyrolysis front; FDS simulation; Temperature distribution; Air entrainment.

1. Introduction

In modern high-rise buildings, polymer materials are widely used in exterior wall design and insulation, but most of these materials are flammable, and the flame will spread rapidly along the surface of the material after being ignited. In the process of flame spread, due to different flame spread rates at different locations, the morphology of the pyrolysis front (the interface between the solid fuel and the combustion flame) is different. In other words, when the exterior wall is on fire, the fire risk may be different in different parts of the building. For example, in 2021, Dalian Triumph International Building caught fire in the home of a resident on the 19th floor, and the flame spread outside the window to ignite the external wall insulation material, which caused the fire and continued to spread downward. Fortunately, the accident did not cause casualties, but caused certain economic losses. Therefore, relevant research on the morphology of pyrolysis front during the flame spread of solid combustibles can provide some theoretical references for building fire protection design and accident rescue work.

In many previous studies on the downward flame spread of solid fuels, the study on the morphology of the pyrolysis front is relatively insufficient, and often only stays in the qualitative description of the phenomenon, lacking a detailed analysis of the formation mechanism. Ayani et al. [1] and Zhao et al. [2] experimentally studied the three-dimensional downward fire propagation behavior of polymethyl methacrylate (PMMA) plate, and the results showed that the pyrolysis front presented an inverted "V" shape in the stable stage. Ma et al. [3], Tu et al. [4], Gong et al. [5] studied the downward flame spread behavior of polyurethane (PU) and PMMA plate with a backboard respectively using calcium silicate and gypsum as backboards. The results all showed that the initial linear shape of the cause before pyrolysis changed into an inverted "V" shape during the downward flame spread process. Carmignani et al. [6] studied the two-dimensional downward fire propagation of PMMA plate (side limited, no backboard), and the results showed that the pyrolysis front was linear. An et al. [7], Luo et al. [8], Yan et al. [9] experimentally studied the effect of U-shaped structure (side limited with backboard) on the downward spreading of expanded

polystyrene (XPS) and PMMA plates, respectively. The results showed that, under the U-shaped structure, the temperature of XPS and PMMA plates decreased significantly. The pyrolysis front of different samples was linear in the whole spreading process. It can be seen that the morphology of the pyrolysis front in the stable stage of downward flame spread on the solid fuel plate can be divided into two types: linear and inverted "V" shape. Under the condition of free downward flame spread, the pyrolysis front must evolve from a straight line to an inverted "V" shape, and after side combustion is suppressed, the pyrolysis front will be straight in the whole process regardless of whether there is a backboard.

In previous experimental studies [10], it was found that the presence of backboard significantly increased the pyrolysis front Angle of 2mm thick PMMA in the combustion stability stage, but had no significant effect on the pyrolysis front Angle of 5mm thick PMMA (see Fig. 1). However, due to the limitations of the experiment, only the velocity boundary layer theory was used to qualitatively describe the reasons for the differences. Therefore, this paper uses FDS to carry out numerical simulation research under the same conditions as the experimental working conditions, quantitatively analyze and reveal the influence mechanism of the backboard on the morphology of the pyrolysis front from the aspects of PMMA surface temperature distribution, flow field and air entraining velocity, and provide data support for the qualitative experiments in the previous work [10].

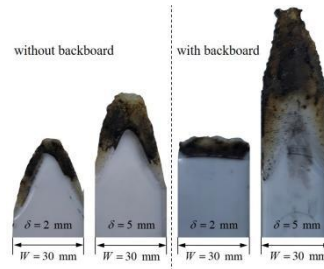


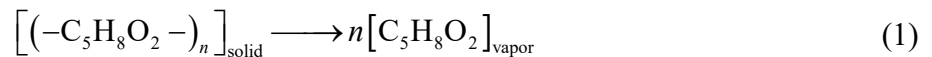
Fig. 1 Variation of pyrolysis front morphology of PMMA during burning stable stage under different conditions

2. Simulation Settings

2.1 Introduction to Simulation software

Fire dynamics simulator (FDS) is a computational fluid dynamics simulation software developed by the National Institute of Standards and Technology. Current studies have shown that FDS is suitable for simulating the flame spread of solid combustibles [11]. In this paper, FDS 6.6.1 was used to simulate the influence of backboard on the morphology of the pyrolysis front during the downward flame spread of PMMA.

The N-S equation is solved by Smagorinsky sublattice model in large eddy simulation. The pyrolysis and combustion of PMMA were simulated by a single step pyrolysis reaction (equivalent to sublimation) combined with a mixed fraction combustion model. In this model, it is assumed that when PMMA reaches a set pyrolysis temperature, methacrylic acid (MMA) monomer vapor is generated immediately, that is:



Next, MMA monomer steam is mixed with air and burned. The mixture fraction combustion model can be expressed as:



In the process of PMMA pyrolysis, combustion and downward spread, the non-scattering gray gas radiation transport equation is used to solve the radiation heat transfer [12, 13].

2.2 Model parameter setting

Referring to the test device [10] of the previous experimental work, a numerical model of the same size was established, as shown in Fig. 2.

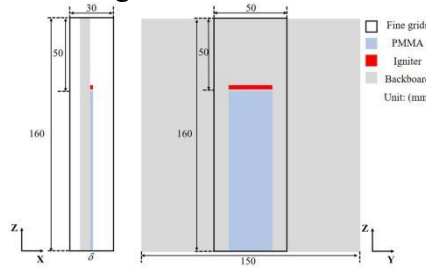


Fig. 2 Model simplification diagram

The width of PMMA is set to 30 mm, the length is set to 110 mm, and other physical and chemical parameters are shown in Table 1. The backboard uses the "Gypsum" of the built-in "Materials" of FDS and sets the thermal conductivity to $0.21 \text{ W} \cdot \text{m}^{-1} \cdot \text{K}^{-1}$, the same as in the experiment. A heat source was set at the top 2 mm of PMMA for ignition, the heat source size was $2 \times 30 \times 3 \text{ mm}$, the surface temperature was set to $1000 \text{ }^{\circ}\text{C}$, and the simulation disappeared after 10 s. Temperature virtual slices and 2D Velocity virtual slices of V (positive direction of Y-axis) and W (positive direction of Z-axis) were set at positions 2 mm, 1 mm and 0 mm away from the PMMA side, respectively, and 3D virtual slices of temperature and V and W-velocity were inserted into the combustion zone to observe the changes of temperature and velocity in the region. The ambient temperature is set to 293 K, the ambient oxygen mass concentration is set to 0.23 and the ambient nitrogen mass concentration is set to 0.77, there is no ambient wind, and all the boundaries of the entire computing domain are set to "Open" to ensure normal mass and energy exchange with the environment. The simulation time was set to 150 s, but the simulation could be stopped when the morphology of the pyrolysis front was observed to remain stable.

Table 1. Partial physicochemical parameters of PMMA

Parameter	Unit	Numerical value	Source
Density	$\text{kg} \cdot \text{m}^{-3}$	1190	Ananth [14]
Specific heat	$\text{kJ} \cdot \text{kg}^{-1} \cdot \text{K}^{-1}$	1.456	Ayani [1]
Heat conductivity coefficient	$\text{W} \cdot \text{m}^{-1} \cdot \text{K}^{-1}$	0.21	Ayani [1]
Emissivity	/	0.85	McGrattan [13]
Pyrolysis temperature	K	673	Ayani [1]
Pyrolysis enthalpy	$\text{kJ} \cdot \text{kg}^{-1}$	1620	Ananth [14]

2.3 Mesh generation

In simulation research, reasonable mesh size is the basis to ensure the accuracy of the results. McGrattan et al. [13] pointed out that the ratio of characteristic flame diameter to mesh size should be satisfied $4 < D^* / l < 16$, which is D^* expressed as:

$$D^* = \left(\frac{\dot{Q}_{\text{hrr}}}{\rho_{\infty} c_p T_{\infty} \sqrt{g}} \right)^{\frac{2}{5}} \quad (3)$$

Where ρ_{∞} , c_p and T_{∞} respectively represent the density, specific heat and temperature of the air, and g represent the acceleration of gravity, taking $9.81 \text{ m} \cdot \text{s}^{-2}$.

As can be seen from equation (3), D^* mainly depends on the heat release rate \dot{Q}_{hrr} of PMMA in the combustion stabilization stage. Assuming no energy loss in the combustion process of PMMA, the heat release rate can be calculated from the mass loss rate in the combustion stability stage [15]:

$$\dot{Q}_{\text{hrr}} = \dot{Q}_{\text{total}} = \dot{m}_{\text{total}} \cdot \Delta H \quad (4)$$

Where, \dot{Q}_{total} is the total heat feedback received per unit time by PMMA in the combustion stability stage, and ΔH represents the combustion heat of PMMA.

In order to adapt the mesh to different working conditions, the mass loss rate of 2mm thick PMMA in the stable combustion stage under the working condition with backboard was taken [10], and the calculated mesh size was between 0.8mm and 2.5mm combined with formula (3) and (4). Rakesh et al. [11] pointed out in their simulation study on two-dimensional downward flame spread of PMMA that in order to accurately capture the flame spread rate, the mesh size of the flame spread direction should be at least 1 mm. Therefore, after comprehensive consideration of time cost and simulation accuracy, this paper adopts discrete grid for simulation, that is, the calculation domain is divided into 5 regions and uniform grids with different accuracy are used, as shown in Fig. 3. Zone (1) is the combustion reaction zone, where PMMA is ignited and pyrolyzed, and the flame spread behavior is also carried out in this region. Therefore, the mesh size of this region is set to 1 mm; The other areas only exchange gas with the combustion zone, so the mesh size is set to 10 mm.

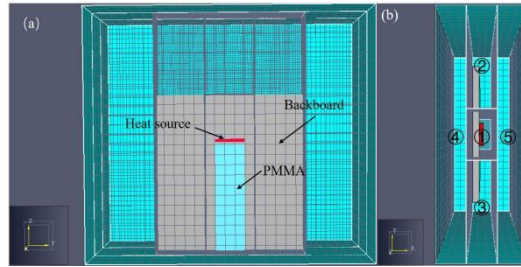


Fig. 3 Calculation area division diagram: (a)front view (b)top view

3. Results and discussion

3.1 Phenomenon observation

Fig. 4 shows the transient changes of the morphology of the pyrolysis front under different working conditions. As can be seen from the figure, after a period of spread, the pyrolysis front of all conditions finally presents an obvious inverted "V" shape, while the condition with a backboard takes a longer time to form a stable inverted "V" shape. The measurement of the leading edge Angle in the stable stage shows that: the pyrolysis leading edge Angle of 2 mm thick PMMA without backboard is significantly smaller than that of the one with backboard, while the pyrolysis leading edge Angle of 5mm thick PMMA has little difference between the two working conditions with and without backboard, but the working condition without backboard is still smaller than that with backboard, which is consistent with the previous experimental observation [10].

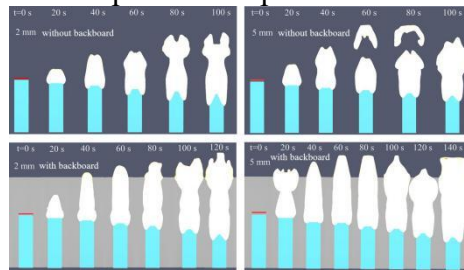


Fig. 4 Variation of pyrolysis front morphology with time

3.2 Effect of backboard on the surface temperature distribution of PMMA

Fig. 5 shows the surface temperature distribution of 5 mm thick PMMA under two conditions with or without backboard at the 12th s of spreading (the 2nd s after the ignition source is removed). In this case, the pyrolysis front is linear. The temperature distribution cloud map shows that the temperature at the edge of PMMA is obviously higher than that in the middle of PMMA under the condition without backboard. In the case of backboard, the temperature difference between the front

edge and the middle is not obvious, but the temperature distribution of the side shows that the temperature of the non-attached side is obviously higher than that of the attached side.

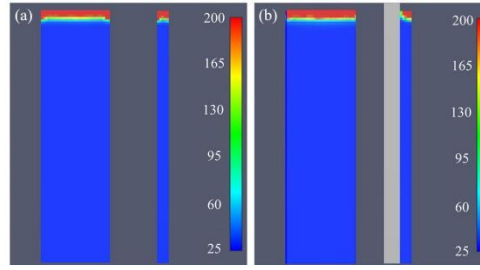


Fig. 5 Cloud image of PMMA surface temperature distribution at pyrolysis front bottom: (a)without backboard (b)with backboard

Fig. 6 shows the front and side surface temperature distributions of PMMA at the bottom of the linear pyrolysis front under different working conditions. The data points in the figure are average values within 2 to 3 seconds. As can be seen from the figure, under the condition without backboard, the temperatures at the front and side edges of PMMA of the two thicknesses are higher than those in the middle. Therefore, after spreading for a period of time, the pyrolysis fronts of the front and side of PMMA show an inverted "V" shape, which is consistent with the experimental phenomenon (see [10]). In the condition with backboard, the temperature of the side attached edge of PMMA of the two thicknesses is lower than that of the non-attached edge, while the temperature distribution of the front side is consistent with that of the condition without backboard. Therefore, after spreading for a period of time, the pyrolysis front of the side and the front side presents a "\ " shape and an inverted "V" shape respectively, and the same phenomenon has been observed in the experiment (see [10]). In addition, by comparing Fig. 6 (c) and (d), it can be found that the presence of a backboard reduces the surface temperature of PMMA of the two thicknesses, which is more obvious when the thickness is 2 mm, indicating that the presence of backboard leads to the decrease of flame spread rate at the edge.

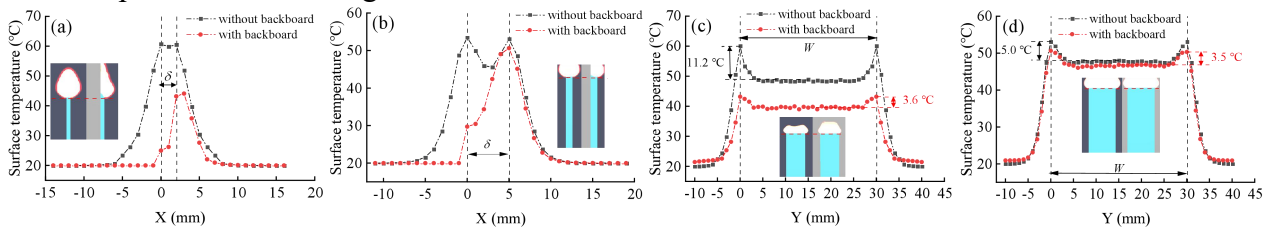


Fig. 6 PMMA surface temperature distribution: (a) $\delta = 2$ mm (b) $\delta = 5$ mm (lateral temperature distribution) (c) $\delta = 2$ mm (d) $\delta = 5$ mm (frontal temperature distribution)

3.3 Influence of backboard on flow field and air entrainment

Because the air enrolling in the X direction is mainly concentrated in the front [7, 16], and the influence of the back plane on the air enrolling is mainly reflected near the back plane. Therefore, this paper only analyzes the change of air velocity in Y and Z directions near the backboard. Slices of Y velocity (V_y) and Z velocity (V_z) combined velocity (V_{yz}) at a distance of 1 mm from the front in the combustion stabilization stage were selected, as shown in the dotted line box in Fig. 7 (a), and plotted as the velocity distribution cloud map and flow diagram. The differences between the two working conditions with or without backboard were compared, and the results were shown in Fig. 8.

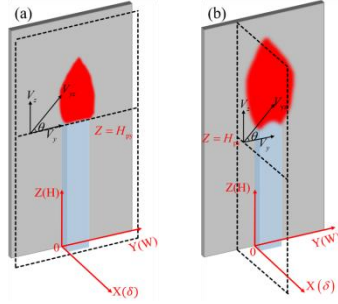


Fig. 7 Simplified diagram of 2D velocity slices at different positions

It can be observed from Fig. 8 that in the condition without backboard, at the pyrolysis front of the sample at the side of the combustion stability stage, air will not only be sucked vertically up from the bottom, but also be sucked up from both sides and merged into the upward air entrainment flow. Relatively speaking, when the backboard is present, the horizontal air enrolling at both sides of the edge pyrolysis front is not obvious, and the overall trend of the flow diagram is closer to the vertical upward, indicating that the backboard does affect the horizontal air enrolling at the edge.

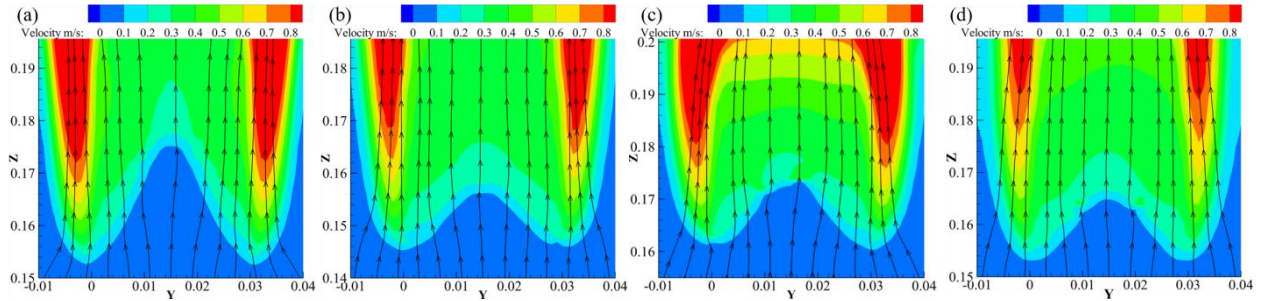


Fig. 8 Velocity distribution and flow diagram at 1 mm from front during burning stable stage:
(a) $\delta=2$ mm, without backboard (b) $\delta=2$ mm, with backboard (c) $\delta=5$ mm, without backboard
(d) $\delta=5$ mm, with backboard

Fig. 9 shows the changes of 2mm thick PMMA with X under two working conditions with or without backboard. It can be seen from the figure that V_y is symmetric with respect to $X=1$ mm under the condition without backboard, and increases with the increase of distance from this point. Under the condition with backboard, V_y slowly increases from 0 at first as the distance from the wall sticking edge increases, and rapidly increases when the sample thickness exceeds 1 mm ($X=3$ mm), indicating that horizontal air enrolling is indeed affected by the velocity boundary layer near the backboard. At the same time, by comparing the V_y in the two conditions with or without backboard, it can be found that the presence of backboard not only reduces V_y in the thickness range, but also reduces V_y in a certain range outside the thickness. However, when the distance increases to a certain value, the V_y in the condition with backboard exceeds that in the condition without backboard.

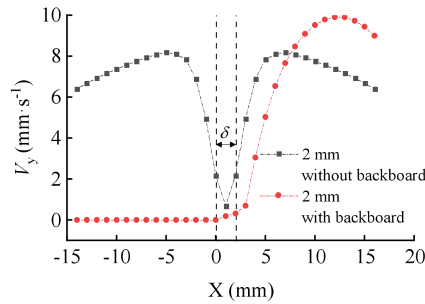


Fig. 9 Lateral air entrainment velocity distribution of 2 mm thick PMMA under conditions with and without backboard

4. Conclusion

In this paper, based on previous experimental studies, the pyrolysis front morphology of 2 mm and 5 mm thick PMMA under two conditions with or without backboard was simulated by FDS, and the reasons for the differences in pyrolysis front morphology were analyzed based on the changes in temperature, flow field and air velocity. The main findings are as follows:

(1) The front pyrolysis front presents an inverted "V" shape in the stable stage under both conditions with and without backboard. Under the condition of backboard, the temperature of the side non-adherent edge is obviously higher than that of the adherent edge, so the pyrolysis front is "\ " shape.

(2) Although the front pyrolysis front in the stable stage is inverted "V" shape, the pyrolysis front Angle in the stable combustion stage with backboard is larger than that in the condition without backboard, and this phenomenon is more obvious at small thickness PMMA.

(3) The presence of the backboard changes the flow field at the edge of PMMA, making the air there closer to the vertical upward, almost parallel to the direction of the combustion plume flow.

Acknowledgements

This work was supported by the National Natural Science Foundation of China under Grant (Nos. 51876088 and 51506082) and the Six Talent Peaks Project of Jiangsu Province of China under Grant (No. XNYQC-005).

References

- [1] Ayani M B, Esfahani J A, Mehrabian R. Downward flame spread over PMMA sheets in quiescent air: Experimental and theoretical studies[J]. *Fire Safety Journal*, 2006, 41(2): 164-169.
- [2] Zhao K, Zhou X D, Liu X Q, et al. Prediction of three-dimensional downward flame spread characteristics over poly(methyl methacrylate) slabs in different pressure environments[J]. *Materials (Basel)*, 2016, 9(11): 1-15.
- [3] Ma X, Tu R, Cheng X D, et al. Sub-Atmospheric pressure coupled with width effect on downward flame spread over energy conservation material polyurethane foam[J]. *Journal of Thermal Science*, 2020, 29: 115-121.
- [4] Tu R, Ma X, Zeng Y, et al. Influences of sub-atmospheric pressure on downward flame spread over typical insulation material with parallel glass curtain wall structure in underground buildings[J]. *Tunnelling and Underground Space Technology*, 2020, 103: 103509.
- [5] Gong J H, Zhou X D, Li J, et al. Effect of finite dimension on downward flame spread over PMMA slabs: Experimental and theoretical study[J]. *International Journal of Heat and Mass Transfer*, 2015, 91: 225-234.
- [6] Carmignani L, Bhattacharjee S. Burn angle and its implications on flame spread rate, mass burning rate, and fuel temperature for downward flame spread over thin PMMA[J]. *Combustion Science and Technology*, 2019, 192(8): 1617-1632.
- [7] An W G, Xiao H H, Sun J H, et al. Effects of sample width and sidewalls on downward flame spread over XPS slabs[J]. *Fire Safety Science*, 2014, 11: 234-247.
- [8] Luo S F, Xie Q Y, Da L H, et al. Experimental study on thermal structure inside flame front with a melting layer for downward flame spread of XPS foam[J]. *Journal of Hazardous Materials*, 2019, 379: 120775.
- [9] Yan W G, Li J T, Shen Y, et al. Experimental investigations on the flame spread of building's vertical U-shape facade[J]. *Journal of Thermal Analysis and Calorimetry*, 2021, 147: 5961-5971.
- [10] Li D Y, Zhao K, Zhou K B, et al. Effects of the backboard on downward flame spread over polymethyl methacrylate[J]. *Journal of Tsinghua University (Science and Technology)*, 2023, 63(5): 783-791.
- [11] Rakesh Ranga H R, Korobeinichev O P, Harish A, et al. Investigation of the structure and spread rate of flames over PMMA slabs[J]. *Applied Thermal Engineering*, 2018, 130: 477-491.

- [12] Wang H Y, Bastien C. Numerical simulation of wind-aided flame spread over horizontal surface of condensed fuel in confined channel[J]. *International Journal on Engineering Performance-Based Fire Codes*, 2007, 9(2): 65-77.
- [13] Mcgrattan K, Forney G, Floyd J E, et al. Fire dynamics simulator (version 4) user's guide [M]. Gaithersburg: NIST special publication, 2010.
- [14] Ananth R, Ndubizu C C, Tatem P A. Burning rate distributions for boundary layer flow combustion of a PMMA plate in forced flow[J]. *Combustion and Flame*, 2003, 135(1-2): 35-55.
- [15] Zhao K, Zhou X D, Yang L Z, et al. Width effects on downward flame spread over poly(methyl methacrylate) sheets[J]. *Journal of Fire Sciences*, 2014, 33(1): 69-84.
- [16] An W G, Wang Z, Xiao H H, et al. Thermal and fire risk analysis of typical insulation material in a high elevation area: Influence of sidewalls, dimension and pressure[J]. *Energy Conversion and Management*, 2014, 88: 516-524.